J. Fluid Mech. (2014), *vol.* 755, *pp.* 50–61. © Cambridge University Press 2014
doi:10.1017/jfm.2014.418

Two-vortex equilibrium in the flow past a flat plate at incidence

Luca Zannetti[1,†] **and Alexandre Gourjii**[2]

[1]DIMEAS, Politecnico di Torino, C.so Duca degli Abruzzi 24, 10129 Torino, Italy

[2]National Technical University of Ukraine'KPI', 37 Pobedy av., 03056 Kiev, Ukraine

(Received 4 April 2014; revised 19 May 2014; accepted 16 July 2014;
first published online 14 August 2014)

The two-dimensional inviscid incompressible steady flow past an inclined flat plate is considered. A locus of asymmetric equilibrium configurations for vortex pairs is detected. It is shown that the flat geometry has peculiar properties compared to other geometries: (i) in order to satisfy the Kutta condition at both edges, which ensures flow regularity, the total circulation and the force acting on the plate must be zero; and (ii) the Kutta condition and the free vortex equilibrium conditions are not independent of each other. The non-existence of symmetric equilibrium configurations for an orthogonal plate is extended to more general asymmetric flows.

Key words: vortex flows, vortex instability, wakes/jets

1. Introduction

According to Meleshko & Aref (2007), Joukowskii (1907) was the first to consider a vortex pair in the steady flow past an orthogonal flat plate. He argued that the Kutta condition, which ensures regular flow at the plate edges, cannot be satisfied if the vortex pair is standing in equilibrium. After that, a controversy arose that lasted for nearly seventy years. Meleshko & Aref (2007) list nine references which alternately rejected and confirmed that result. The dispute was closed by Smith & Clark (1975), who analytically proved that Joukowskii was right.

The detection of equilibrium configurations of point vortices in two-dimensional flows past bluff bodies is of interest beyond the general theoretical one. For instance, as described by Gallizio *et al.* (2010) and references therein, point vortices can be continued into vortex patches *á la* Prandtl–Batchelor and their equilibria are relevant to flow control at high Reynolds number *Re*.

The problem of the existence of vortex pair equilibria in a regular flow past a flat plate is considered here for the general case of asymmetric flow. The asymmetry in the flow is created by the inclination of the plate, or by an asymmetric vortex pair. Loci of equilibrium configurations exist when the plate is not orthogonal to the flow, that is, when the angle of attack α is non-zero. As α goes to zero the solution becomes symmetric, but the distances from the plate to the vortices go to infinity. This implies that not only do two-vortex equilibria not exist, as shown by Smith & Clark (1975), but also asymmetric equilibria cannot be realized at $\alpha = 0$.

† Email address for correspondence: luca.zannetti@polito.it

https://doi.org/10.1017/jfm.2014.418 Published online by Cambridge University Press

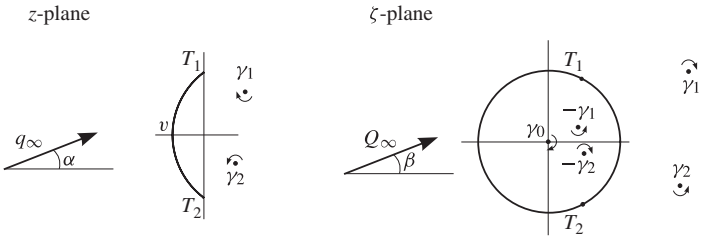


FIGURE 1. Schematic of physical and transformed planes.

As shown below, the flat geometry involves aspects which set it apart from other two-dimensional geometries and which might not have been anticipated. Unlike other geometries, the flow regularity at the flat-plate edges, that is the enforcement of the Kutta condition, implies a zero global circulation and a relationship between the vortex equilibrium equations. Moreover, continuation arguments as in Gallizio *et al.* (2010), suggest that the topology of the wake past a flat plate is incompatible with the asymptotic Batchelor flow model.

2. Governing equations

In this section, we derive the governing equations for more general geometries. We use the same flow model as in Elcrat, Ferlauto & Zannetti (2014), which refers to results presented at the IUTAM Symposium on Vortex Dynamics held in 2013 at Fukuoka (Japan), where two standing point vortices are used to model the wake past bodies with two sharp edges.

In general, for any body geometry, the flow can be expressed by conformal mapping. A schematic is shown in figure 1, pertinent to a body shaped as an arc of a circle. Let $z=f(\zeta)$ be the mapping that transforms the exterior of the unit circle of the complex ζ-plane onto the exterior of the z-plane body, such that $f(\infty)=\infty$. The complex potential, expressed in the ζ-plane, is

$$w = Q_\infty \left(\mathrm{e}^{-\mathrm{i}\beta}\zeta + \frac{\mathrm{e}^{\mathrm{i}\beta}}{\zeta} \right) + \frac{1}{2\pi\mathrm{i}} \left(\gamma_0 \log \zeta + \sum_{j=1}^{2} \gamma_j \log \frac{\zeta - \zeta_j}{\zeta - 1/\bar{\zeta}_j} \right), \tag{2.1}$$

where γ_j, ζ_j $(j=1,2)$ are the circulations and locations of the free vortices, respectively, $Q_\infty \exp(-\mathrm{i}\,\beta) = q_\infty \exp(-\mathrm{i}\,\alpha)(\mathrm{d}z/\mathrm{d}\zeta)_\infty$, with q_∞ and α being the flow velocity and incidence at infinity on the physical plane, and γ_0 is the total circulation, that is, the circulation along a line which encloses the body and all vortices.

The complex velocity $\dot{\bar{z}}$ of a flow particle is $\dot{\bar{z}} = (\mathrm{d}w/\mathrm{d}\zeta)/(\mathrm{d}z/\mathrm{d}\zeta)$, with

$$\frac{\mathrm{d}w}{\mathrm{d}\zeta} = Q_\infty \left(\mathrm{e}^{-\mathrm{i}\beta} - \frac{\mathrm{e}^{\mathrm{i}\beta}}{\zeta^2} \right) + \frac{1}{2\pi\mathrm{i}} \left[\frac{\gamma_0}{\zeta} + \sum_{j=1}^{2} \gamma_j \left(\frac{1}{\zeta - \zeta_j} - \frac{1}{\zeta - 1/\bar{\zeta}_j} \right) \right], \tag{2.2}$$

and the complex velocity $\dot{\bar{z}}_j$ of a free vortex is

$$\dot{\bar{z}}_j = \lim_{z \to z_j} \left(\frac{\mathrm{d}w}{\mathrm{d}z} - \frac{\gamma_j}{2\pi\mathrm{i}} \frac{1}{z - z_j} \right), \tag{2.3}$$

https://doi.org/10.1017/jfm.2014.418 Published online by Cambridge University Press

that is

$$\dot{\bar{z}}_j = \left(\bar{\zeta}'_j - \frac{\gamma_j}{4\pi \mathrm{i}} \frac{\mathrm{d}}{\mathrm{d}\zeta_j} \log \frac{\mathrm{d}z_j}{\mathrm{d}\zeta_j}\right) \Big/ \frac{\mathrm{d}z_j}{\mathrm{d}\zeta_j} \tag{2.4}$$

where

$$\begin{aligned} \bar{\zeta}'_j &= \lim_{\zeta \to \zeta_j} \left(\frac{\mathrm{d}w}{\mathrm{d}\zeta} - \frac{\gamma_j}{2\pi \mathrm{i}} \frac{1}{\zeta - \zeta_j}\right) \\ &= Q_\infty \left(\mathrm{e}^{-\mathrm{i}\beta} - \frac{\mathrm{e}^{\mathrm{i}\beta}}{\zeta_j^2}\right) + \frac{1}{2\pi \mathrm{i}} \left[\frac{\gamma_0}{\zeta_j} - \gamma_j \frac{1}{\zeta_j - 1/\bar{\zeta}_j} + \gamma_k \left(\frac{1}{\zeta_j - \zeta_k} - \frac{1}{\zeta_j - 1/\bar{\zeta}_k}\right)\right], \end{aligned} \tag{2.5}$$

with $j = 1, 2$ and $k = 2, 1$. Relationship (2.4) between $\dot{\bar{z}}_j$ and $\bar{\zeta}'_j$ expresses how the vortex velocity transforms under conformal mapping and is generally referred to as the 'Routh rule' (see, for instance, Clements 1973).

We first consider a body shaped as an arc of a circle. With reference to figure 1, the arc edges are located at $z_T = \pm \mathrm{i}$ and the vertex at $z_V = b$. The Jukowskii transformation

$$z = \frac{1}{2}\left(|\mathrm{i} - b|\zeta + b - \frac{1}{|\mathrm{i} - b|\zeta + b}\right) \tag{2.6}$$

maps the arc onto the unit circle of the ζ-plane.

The presence of two trailing edges requires that a regular flow has to satisfy two Kutta conditions:

$$\left(\frac{\mathrm{d}w}{\mathrm{d}\zeta}\right)_{\zeta_{T_1}} = \left(\frac{\mathrm{d}w}{\mathrm{d}\zeta}\right)_{\zeta_{T_2}} = 0. \tag{2.7}$$

3. Degrees of freedom

Once reference values of length and velocity are set, (2.1) shows that the flow depends on eight real parameters: the angle of attack α, the circulations γ_0, γ_1, γ_2 and the complex locations ζ_1, ζ_2 of the free vortices. If the vortices are required to stand in equilibrium, the degrees of freedom reduce to four, for the vortex complex velocities (2.4) have to be zero, i.e. $\dot{\bar{z}}_j = 0$. If two Kutta conditions are to be satisfied, two additional degrees of freedom are subtracted from the flow. In conclusion, for a given angle of attack α, in general the flow past a body with two sharp edges is expected to have a single degree of freedom.

In Elcrat *et al.* (2014), this degree of freedom is represented by the global circulation γ_0, whose free selection results in different wake configurations. As an example, figure 2 shows two different flow fields past an arc of a circle, that are obtained using the same far-field boundary conditions (α) but different global circulations γ_0. Figure 2(*a*) shows the symmetric streamline pattern relevant to a zero global circulation γ_0, while figure 2(*b*) shows the asymmetric pattern obtained for $\gamma_0 = -0.38$. A schematic of the streamline pattern of figure 2(*b*) is presented in figure 3.

The flow patterns shown in figure 2 can be regarded as inviscid models of steady wakes past bluff bodies. According to Batchelor (1956), in the limit as $Re \to \infty$, the wake should be formed by two vortex patches. By desingularizing the point vortices into vortex patches, as in Elcrat *et al.* (2000), the above solutions could be considered as the seeds from which the Batchelor flow solutions grow. In this respect, as pointed out in Elcrat *et al.* (2014), the two patterns in the figure are not equivalent. Let the

https://doi.org/10.1017/jfm.2014.418 Published online by Cambridge University Press

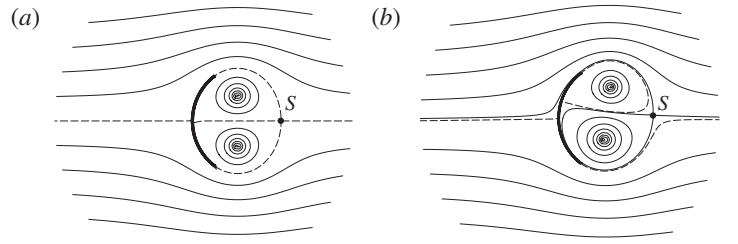


FIGURE 2. Flow past an arc of a circle ($b = -0.5$) at $\alpha = 0$. (*a*) $\gamma_0 = 0$, $\gamma_1 = -\gamma_2 = -7.01$, $z_1 = \bar{z}_2 = 0.49 + \mathrm{i}\,0.56$. (*b*) $\gamma_0 = -0.38$, $\gamma_1 = -6.99$, $\gamma_2 = 7.63$, $z_1 = 0.64 + \mathrm{i}\,0.69$, $z_2 = 0.50 - \mathrm{i}\,0.47$.

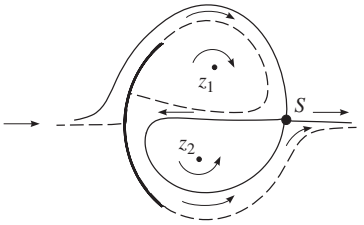


FIGURE 3. Schematic of the flow-pattern of figure 2(*b*).

wake be defined as the region bounded by the separating streamlines (dashed lines): in figure 2(*a*) these streamlines join at the stagnation point S and bound a closed wake, while in figure 2(*b*) they do not join and the wake is open. According to the Batchelor flow solution (Batchelor 1956), only the closed topology (figure 2*a*) is allowed because an embedded vortex patch, such as the one replacing the lower vortex in figure 2(*b*), would be surrounded by a potential flow and would violate the maximum principle for vorticity (see Lugt 1985).

The flow past a flat plate is an exception. Below we show that for a flat plate the satisfaction of the Kutta conditions requires that, for any angle of attack α, the global circulation has to be zero, that is $\gamma_0 = 0$. According to the above arguments, one would expect that this flow has no degrees of freedom and that the number of solutions should be finite or zero. The above cited non-existence of solution for a symmetric normal plate ($\alpha = 0$, $\gamma_0 = 0$) seems to confirm this conclusion. On the contrary, we show that the flow past an inclined flat plate still retains one degree of freedom, that is, that there is a locus of infinite equilibrium configurations which satisfy the Kutta conditions, all with $\gamma_0 = 0$.

Consider the force $L = L_x - \mathrm{i}\,L_y$ acting on the plate and the Magnus forces $M_j = M_{j_x} - \mathrm{i}\,M_{j_y}$ exerted on the point vortices, where the subscripts x, y denote x, y components. The Magnus forces

$$M_j = \mathrm{i}\,\gamma_j \dot{\bar{z}}_j \tag{3.1}$$

are non-zero for vortices which are held to stand in non-equilibrium locations, where $\dot{\bar{z}}_j$ (2.4) is the velocity they would have if freely drifting with the stream. The resultant force $F = F_x - \mathrm{i}\,F_y$ on the plate and vortices can be obtained by applying the steady-state Blasius formula to a closed line c which includes the plate and

https://doi.org/10.1017/jfm.2014.418 Published online by Cambridge University Press

vortices; according to the residue theorem, it yields

$$F = L + \sum^{N} M_j = (\mathrm{i}/2) \oint_c (\mathrm{d}w/\mathrm{d}\zeta)^2 (\mathrm{d}\zeta/\mathrm{d}z)\, \mathrm{d}\zeta = \mathrm{i}\, q_\infty\, \mathrm{e}^{-\mathrm{i}\alpha} \gamma_0, \tag{3.2}$$

where N is the number of point vortices. If the vortices are standing in equilibrium, the Magnus forces are zero and the force L is orthogonal to the flow velocity at infinity. As shown, for instance, by Katz & Plotkin (2001), the force L is the result of the pressure acting on the plate sides, which provides a contribution orthogonal to the plate, and of the 'suction forces', which are parallel to the plate and are due to the flow singularities that occur on the edges when the Kutta condition is not satisfied. This yields the following statement:

If the Kutta condition is satisfied on both edges, the suction contributions are zero and the force L is orthogonal to the plate. As a consequence, only $L = 0$ *is possible and, according to* (3.2), $\gamma_0 = 0$.

Saffman & Sheffield (1977) found that for a single standing vortex ($N = 1$) at any incidence there is no equilibrium configuration that satisfies the Kutta condition at both edges. This result is confirmed by inspection of equation (2.7) which for $N = 1$, $\gamma_0 = 0$ and for any value of the vortex location ζ_1, becomes a set of two incompatible linear equations for the single unknown γ_1.

The degree of freedom seemingly lost because of the constraint $\gamma_0 = 0$ is recovered by considering that for a flat plate the vortex equilibrium equations ($M_j = 0$) and the Kutta conditions are not independent. In any flow configuration, whether or not in equilibrium, when $\gamma_0 = 0$, (3.2) yields $F = 0$, that is, $L = -\sum^{N} M_j$. When the Kutta conditions are satisfied L is orthogonal to the plate. For a plate located on the imaginary axis, $L_y = 0$, that is $\sum^{N} M_{j_y} = 0$. The latter is a relationship between the Magnus forces which results from the fulfillment of the Kutta conditions.

Here we study the case of two vortices ($N = 2$). Let the plate be placed on the imaginary axis by setting $b = 0$ in the mapping (2.6), and let the flow be normalized by taking the velocity at infinity q_∞ as reference velocity and the half-length of the plate as reference length. Once γ_0 is set to zero, for a given angle of attack α the flow depends on six parameters, namely $\gamma_1, \gamma_2, \rho_1, \vartheta_1, \rho_2, \vartheta_2$, where

$$\zeta_1 = \rho_1\, \mathrm{e}^{\mathrm{i}\,\vartheta_1}, \quad \zeta_2 = \rho_2\, \mathrm{e}^{\mathrm{i}\,\vartheta_2} \tag{3.3a,b}$$

are the vortex locations on the ζ-plane. The equilibrium configurations are solutions of the system of five independent equations which express fulfillment of the Kutta conditions and vortex equilibrium. In fact, in addition to the two Kutta conditions (2.7), the vortex equilibrium can be expressed in terms of zero Magnus forces, that is, $M_1 = M_2 = 0$. Since, as stated above, the fulfillment of the Kutta condition implies $\mathrm{Im}(M_1) = -\mathrm{Im}(M_2)$, the system can be closed by adding to (2.7) the three real equations

$$\mathrm{Re}(M_1) = 0, \quad \mathrm{Re}(M_2) = 0, \quad \mathrm{Im}(M_1) = 0, \tag{3.4a–c}$$

which are sufficient to ensure vortex equilibrium.

4. Examples

According to the above analysis, for given far-field boundary conditions the system (2.7), (3.4) has one degree of freedom, which can be expressed by the free selection of one of the six parameters $\gamma_1, \gamma_2, \rho_1, \vartheta_1, \rho_2, \vartheta_2$. In the following examples we

https://doi.org/10.1017/jfm.2014.418 Published online by Cambridge University Press

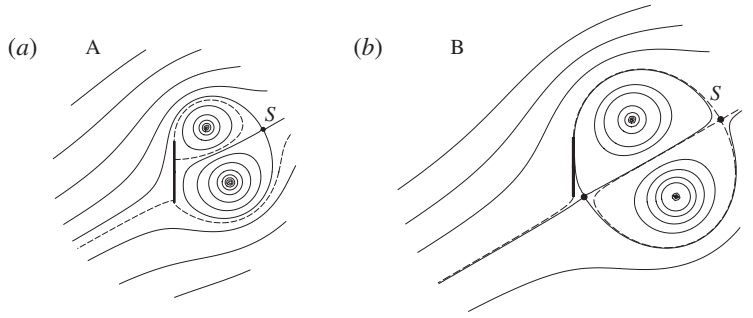


FIGURE 4. Streamlines for $\alpha = 30°$. (*a*) Case A ($\vartheta_1 = 0.86$): $z_1 = 1.05 + \mathrm{i}\,1.43$, $z_2 = 1.80 - \mathrm{i}\,0.34$, $\gamma_1 = -11.24$, $\gamma_2 = 12.87$. (*b*) Case B ($\vartheta_1 = 0.64$): $z_1 = 1.97 + \mathrm{i}\,1.59$, $z_2 = 3.45 - \mathrm{i}\,1.01$, $\gamma_1 = -18.72$, $\gamma_2 = 18.87$.

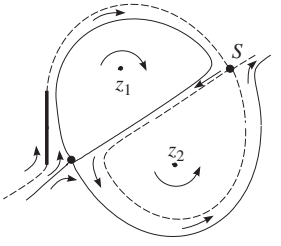


FIGURE 5. Schematic of the flow pattern of figure 4(*b*), case B.

will select either ρ_1 or ϑ_1. Equilibrium configurations have been obtained by means of the Newton method for different values of the angle of attack α. Two numerical procedures, based on in-house FORTRAN codes and on the *Mathematica* software (Version 9.0, Wolfram Research, Inc.), have been used to cross-check the results.

An example of a solution is shown in figure 4, where streamline patterns are presented for $\alpha = 30°$ and for two values of the parameter ϑ_1, that is $\vartheta_1 = 0.86$ (case A) and $\vartheta_1 = 0.64$ (case B). Figure 5 shows a schematic of the streamline pattern of case B. The locus of equilibrium locations for $\alpha = 30°$ is shown in figure 6 for the range $0.60 \leqslant \vartheta_1 \leqslant 1.02$. The patterns for cases A and B are topologically different. The pattern for A is typical of a flow past a bluff body which separates at both edges, while in B the lower edge acts as a leading edge with a smoothly approaching flow. In case A the Kutta condition plays its proper role of an inviscid asymptotic model for viscous separation on a sharp edge, while in B it ensures smoothness to an incoming flow in a less physically grounded way.

The topology of the streamline pattern of case A is the same as for the schematic shown in figure 3: the separating streamlines do not join up at the stagnation point S and, as a consequence, do not bound a closed wake. As in Elcrat *et al.* (2014), the lack of wake closure can be detected by the difference between the stream-function value at the stagnation point S and at the plate $\Delta\psi = \psi_S - \psi_0$. Case B has been obtained by choosing the value of the free parameter ϑ_1 such that $\Delta\psi = 0$ but, as noted above, the flow pattern no longer has the topology of a wake past a bluff body. The non-existence of a closed-wake solution for $\alpha = 30°$ can also be inferred from figure 7(*a*), where the y-component of the flow velocity at the lower edge, v_{T_2}, and

https://doi.org/10.1017/jfm.2014.418 Published online by Cambridge University Press

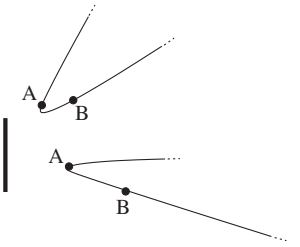


FIGURE 6. Equilibrium manifold for $\alpha = 30°$. Points A and B are relevant to figure 4.

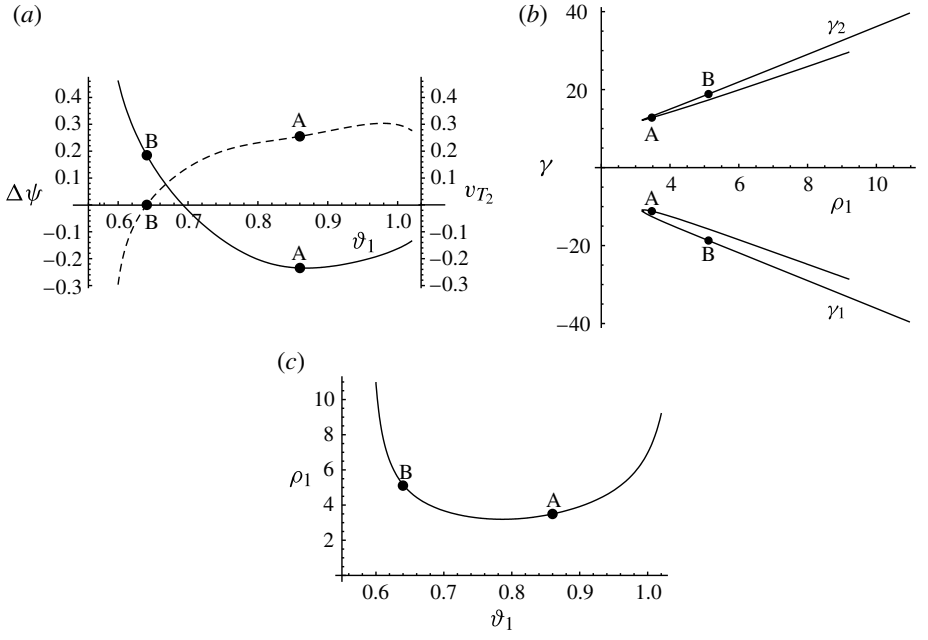


FIGURE 7. Angle of attack $\alpha = 30°$: (*a*) $\Delta\psi$ (dashed line) and v_{T_2} (solid line) versus ϑ_1; (*b*) vortex circulations γ_1 and γ_2 versus ρ_1; (*c*) ρ_1 versus ϑ_1. A and B refer to figure 4.

$\Delta\psi$ are plotted versus ϑ_1. The 'bluff-body regime', that is, the flow that separates at the edges, corresponds to the range with $v_{T_2} < 0$; as shown by figure 7(*a*), in that range $\Delta\psi \neq 0$. The flow velocity v_{T_2} at the lower edge has been computed by the equation

$$v_{T_2} = -\mathrm{Im}\left(\lim_{\zeta\to -\mathrm{i}} \frac{\mathrm{d}w/\mathrm{d}\zeta}{\mathrm{d}z/\mathrm{d}\zeta}\right) = \mathrm{Im}\left(\frac{\mathrm{d}^2 w}{\mathrm{d}\zeta^2}\zeta^3\right)_{\zeta=-\mathrm{i}}. \tag{4.1}$$

Figure 7(*b*) shows the vortex strengths γ_1, γ_2 as functions of the parameter ρ_1 along the equilibrium manifold and illustrates how the vortex circulations increase with the distance from the plate.

In figure 7(*c*), the distance ρ_1 of the upper vortex from the origin of the ζ-plane has been plotted versus ϑ_1. It shows that there is a minimum value $\rho_{1_{min}} = 3.1926$ below which our numerical procedure has been unable to find other equilibrium configurations.

https://doi.org/10.1017/jfm.2014.418 Published online by Cambridge University Press

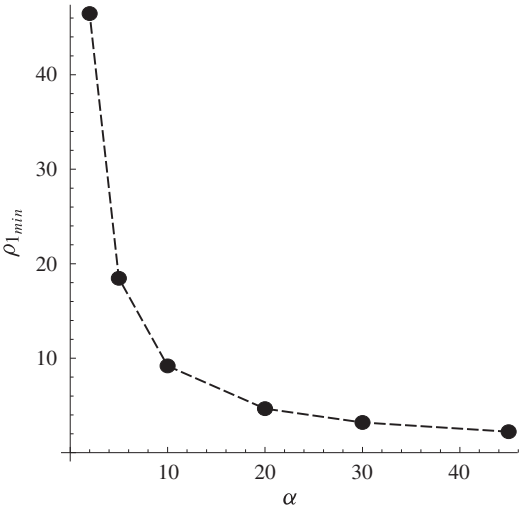


FIGURE 8. Minimum ρ_1 versus angle of attack α.

In addition to $\alpha = 30°$, we tested other angles of attack, namely: $\alpha = 2°, 5°, 10°, 20°, 45°$. For all of these angles of attack the flow features are qualitatively the same as figures 4 and 7 for $\alpha = 30°$.

In figure 8 $\rho_{1_{min}}$ is plotted versus α. The results suggest that for any angle of attack α there exists a minimum value $\rho_{1_{min}}$ which tends to infinity as α tends towards zero. This behaviour confirms the result that for an orthogonal flat plate there exists no standing vortex pair which satisfies the Kutta conditions at the edges (Smith & Clark 1975).

The tendency of $\rho_{1_{min}}$ to infinity as α tends to zero is confirmed by figure 9, where the equilibrium manifold for an almost orthogonal plate ($\alpha = 2°$) is compared to the manifold corresponding to $\alpha = 45°$. An interesting outcome of the figure is that the equilibrium manifold tends to be symmetric as α tends to zero. In their non-existence proof, Smith & Clark (1975) considered the flow configuration as symmetric. The above analysis of the degrees of freedom of the flow seems to indicate that asymmetric solutions might in fact exist as, for instance, in the case of a flow past a circular cylinder (e.g. Iosilevskii & Seginer 1994; Elcrat *et al.* 2014). Our results suggest otherwise: asymmetric solutions are unlikely to exist as they become symmetric as α tends to zero, and thus there is no solution for $\alpha = 0$.

Figure 10(*a*) shows that the wake closure behaviour for $\alpha = 2°$ is similar to the behaviour shown by figure 7(*a*) for $\alpha = 30°$, that is, in the bluff-body regime ($v_{T_2} < 0$), the wake never closes ($\Delta\psi \neq 0$). We have verified this behaviour for the other tested angles of attack α also.

Figure 10(*b*) shows the streamline pattern for $\rho_1 = \rho_{1_{min}}$. The corresponding values of $\Delta\psi$ and v_{T_2} are marked by dots in figure 10(*a*). The lack of wake closure is not visible at the scale of the figure and the pattern appears similar to that of a free vortex pair. Indeed, if the minimum vortex distance from the plate ($|z_1|_{min}$) is selected as reference length instead of the half-plate length, the figure suggests that as $\alpha \to 0$ the plate vanishes into the front stagnation point of a vortex-pair flow.

https://doi.org/10.1017/jfm.2014.418 Published online by Cambridge University Press

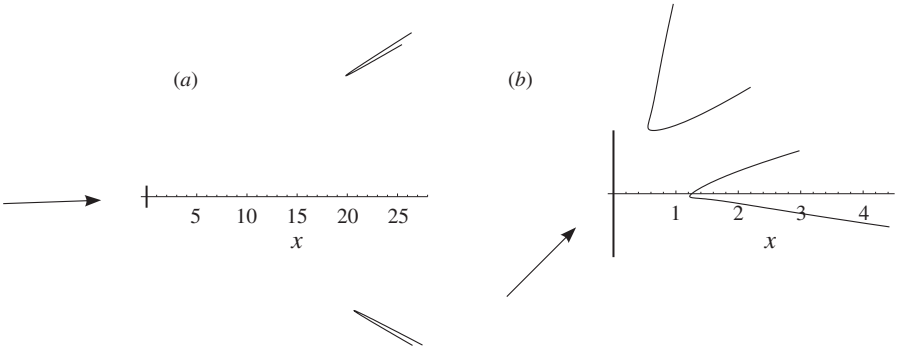


FIGURE 9. Equilibrium manifold for (*a*) $\alpha = 2°$ and (*b*) $\alpha = 45°$.

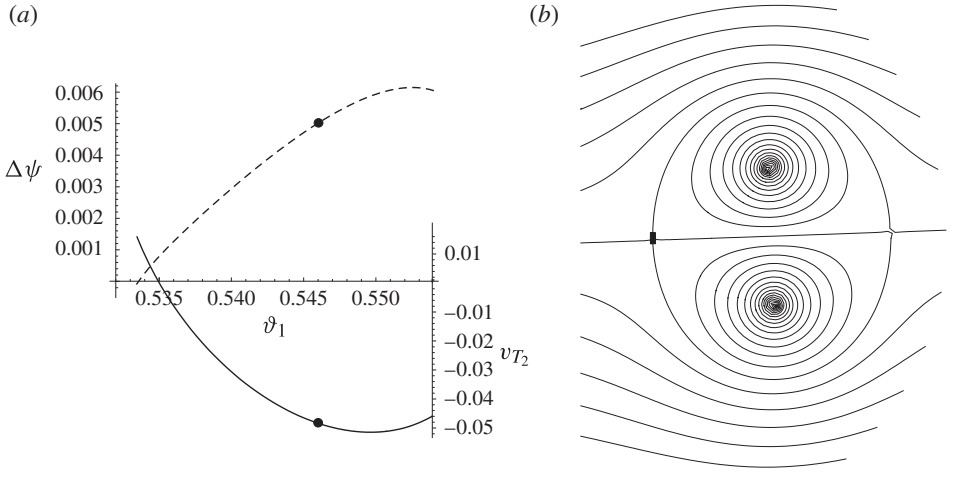


FIGURE 10. Angle of attack $\alpha = 2°$. (*a*) $\Delta\psi$ (dashed line) and v_{T_2} (solid line) versus ϑ_1. The dots refer to $\rho_1 = \rho_{1_{min}}$. (*b*) Streamlines for $\rho_1 = \rho_{1_{min}} = 46.47$, $\vartheta_1 = 0.545$, $\rho_2 = 47.18$, $\gamma_1 = -147.14$, $\gamma_2 = 147.15$. The black rectangle represents the vanishing plate.

5. Linear stability

In order to study the stability of the detected equilibria, we rewrite (2.4) as

$$\gamma_j \dot{\bar{z}}_j = \gamma_j \dot{x}_j - \mathrm{i}\,\gamma_j \dot{y}_j = \frac{\partial K}{\partial y_j} + \mathrm{i}\,\frac{\partial K}{\partial x_j} \tag{5.1}$$

where the Kirchhoff–Routh path function $K(x_j, y_j)$, with $j = 1, 2$, has been introduced (see, for instance Saffman 1992). Equation (5.1) has the form of a two-degree-of-freedom Hamiltonian system with K being the Hamiltonian and $(\sqrt{|\gamma_j|}\mathrm{sgn}(\gamma_j)\, x_j, \sqrt{|\gamma_j|}\mathrm{sgn}(\gamma_j)\, y_j)$ the canonical variables. An exhaustive treatment of point-vortex Hamiltonian dynamics has been provided by Newton (2000); more recent developments have been given by Crowdy & Marshall (2005), Zannetti (2006) and Vasconcelos, Moura & Schakel (2011).

https://doi.org/10.1017/jfm.2014.418 Published online by Cambridge University Press

Let H be the Hamiltonian of the vortex system on the transformed ζ-plane. Lin (1941) has shown that K can be derived from H according to the relationship

$$K = H + \frac{1}{4\pi}\sum_{j=1}^{2}\gamma_j^2 \log\left|\frac{\mathrm{d}z_j}{\mathrm{d}\zeta_j}\right|, \tag{5.2}$$

where

$$\begin{aligned} H \;=\; & \sum_{j=1}^{2}\gamma_j\left[Q_\infty(\eta_j\cos\beta-\xi_j\sin\beta)\left(1-\frac{1}{\xi_j^2+\eta_j^2}\right)+\frac{\gamma_j}{4\pi}\log(\xi_j^2+\eta_j^2-1)\right] \\ & -\frac{\gamma_1\gamma_2}{4\pi}\log\frac{(\xi_1-\xi_2)^2+(\eta_1-\eta_2)^2}{(\xi_1\xi_2+\eta_1\eta_2-1)^2+(\xi_1\eta_2-\xi_2\eta_1)^2}, \end{aligned} \tag{5.3}$$

with $\xi+\mathrm{i}\,\eta=\zeta$.

Following Zannetti & Franzese (1994), it is convenient to avoid the inversion of the mapping $z=f(\zeta)$ and to express K as an explicit function of $(\xi_j,\ \eta_j)$. Equation (5.1) then becomes

$$\gamma_j\dot{\bar{\zeta}}_j=\gamma_j\dot{\xi}_j-\mathrm{i}\gamma_j\dot{\eta}_j=\left(\frac{\partial K}{\partial\eta_j}+\mathrm{i}\,\frac{\partial K}{\partial\xi_j}\right)\Big/J_j, \tag{5.4}$$

where the Jacobian $J_j=|\mathrm{d}z_j/\mathrm{d}\zeta_j|^2$ and $j=1,2$.

The linear stability analysis consists of computing the eigenvalues of the stability matrix $\boldsymbol{A}$ which is associated with the first variation of system (5.4).

The equilibrium perturbation expressed by the first variation consists of a perturbation of the vortex locations while keeping the vortex circulations unaltered. In so doing, the Kutta condition is violated by the perturbation and, from a physical point of view, vortex shedding is expected to be triggered at the plate edges. For the sake of simplicity and as argued by Cai, Liu & Luo (2003), this effect is neglected here.

As a consequence of the Hamiltonian character of system (5.4), the eigenvalues λ of $\boldsymbol{A}$ can only come in real pairs ($\lambda=\pm a,\ a\in\mathbb{R}$), imaginary pairs ($\lambda=\pm\mathrm{i}\,b,\ b\in\mathbb{R}$) and complex quadruplets ($\lambda=\pm a\pm\mathrm{i}\,b,\ a,b\in\mathbb{R}$) (see Arnold 1991). Indeed, the quartic characteristic equation expressing the eigenvalues is biquadratic for any two-degree-of-freedom Hamiltonian system; applying the Cayley–Hamilton theorem (see Gantmacher 1966) gives the result

$$\lambda^4-\tfrac{1}{2}\mathrm{tr}\,(\boldsymbol{AA})\,\lambda^2+\det(\boldsymbol{A})=0. \tag{5.5}$$

Along the equilibrium manifolds detected above, (5.5) yields two real and two imaginary pairs of eigenvalues λ. Since there is a real positive eigenvalue, all the detected equilibrium configurations are unstable. Note that the absolute values of the real eigenvalues are rather small. For instance, the eigenvalues pertinent to the configurations labelled A and B in figure 6 are $\lambda_{1,2}=\pm\mathrm{i}\,0.27$, $\lambda_{3,4}=\pm3.28\times10^{-5}$ and $\lambda_{1,2}=\pm\mathrm{i}\,0.095$, $\lambda_{3,4}=\pm1.57\times10^{-4}$, respectively. This behaviour is typical of the straight geometry of the plate. For instance, the eigenvalues pertinent to the equilibrium configurations past the arc of a circle shown in figure 2(*a*,*b*) are $\lambda_{1,2}=\pm\mathrm{i}\,0.87$, $\lambda_{3,4}=\pm0.66$ and $\lambda_{1,2}=\pm\mathrm{i}\,0.77$, $\lambda_{3,4}=\pm0.59$ respectively, hence much larger real eigenvalues than for the straight flat plate. This can be explained by the fact that the real roots of equation (5.5)

$$\lambda_{3,4}^2=\mathrm{tr}(\boldsymbol{AA})/4+\sqrt{\mathrm{tr}(\boldsymbol{AA})^2/16-\det(\boldsymbol{A})} \tag{5.6}$$

https://doi.org/10.1017/jfm.2014.418 Published online by Cambridge University Press

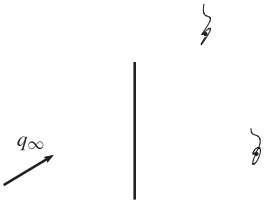


FIGURE 11. Vortex trajectories resulting from a perturbation of the equilibrium configuration A of figure 4 ($\alpha = 30°$, $\vartheta_1 = 0.86$).

(tr($\boldsymbol{AA}$) < 0, det($\boldsymbol{A}$) < 0) are non-zero because of the frozen vortex circulation assumption, which determines a small, non-zero value of det($\boldsymbol{A}$). Indeed, if the intensities of the perturbed vortices were adjusted to satisfy the Kutta condition at the edges, the rank of $\boldsymbol{A}$ would drop to three as a consequence of the relationship $\mathrm{Im}(M_1) = -\mathrm{Im}(M_2)$ presented in § 3, which yields $\delta\dot{x}_1 = -\gamma_2/\gamma_1\,\delta\dot{x}_2$, and det($\boldsymbol{A}$) would be zero.

Numerical evidence of the equilibrium instability is illustrated in figure 11, which shows the initial part of the vortex trajectories following a small perturbation of the configuration A of figure 6.

6. Concluding remarks

The regularity of the steady flow past a flat plate at incidence can be achieved by a minimum of two vortices which stand in equilibrium and satisfy the Kutta conditions at the plate edges.

There is a locus of such vortex pairs for any angle of attack α. The minimum distance of the vortex pair from the plate depends on the angle of attack $|\alpha|$ and tends to infinity as $|\alpha| \to 0$, that is, for a plate orthogonal to the flow. This result is consistent with the Smith & Clark (1975) proof of non-existence of symmetric equilibrium configurations for orthogonal plates and suggests that asymmetric equilibrium configurations do not exist either.

For the flat geometry, the regularity of flows with any number $N \geqslant 2$ of standing vortices implies that the force L acting on the plate is zero. This result applies to any regular inviscid flow field with a compact support for vorticity. For instance, it applies to the growing vortex patches which can be obtained by desingularizing the point vortices (as in Elcrat *et al.* 2000).

In the bluff-body regime, that is, for a flow separating at both edges, let the wake be defined as the region bounded by the separating streamlines. In the range $2° \leqslant \alpha \leqslant 45°$ the wake is not closed. This suggests an infinite wake as $Re \to \infty$. In this case the vorticity support is not compact and the force acting on the plate can be different from zero.

Linear stability analysis shows that the detected equilibria are unstable.

Acknowledgements

The subject of this paper was suggested to the authors by the late Professor V. Meleshko shortly before his untimely passing. We dedicate this work to his memory. Moreover, we are grateful to Dr P. Franzese (Ecology and Environment, Inc.), Professor A. Iollo (Université Bordeaux 1) and Professor K. Miller (Wichita State University) for insightful discussions and their suggestions.

https://doi.org/10.1017/jfm.2014.418 Published online by Cambridge University Press

REFERENCES

ARNOLD, V. I. 1991 *Mathematical Methods of Classical Mechanics*. Springer.

BATCHELOR, G. K. 1956 A proposal concerning laminar wakes behind bluff bodies at large Reynolds number. *J. Fluid Mech.* **1**, 388–398.

CAI, J., LIU, F. & LUO, S. 2003 Stability of symmetric vortices in two dimensions and over three-dimensional slender conical bodies. *J. Fluid Mech.* **480**, 65–94.

CLEMENTS, R. R. 1973 An inviscid model of two-dimensional vortex shedding. *J. Fluid Mech.* **57**, 321–336.

CROWDY, D. G. & MARSHALL, J. S. 2005 Analytical formulae of the Kirchhoff–Routh path function in multiply connected domains. *Proc. R. Soc. Lond.* A **461** (2060), 2477–2501.

ELCRAT, A., FERLAUTO, M. & ZANNETTI, L. 2014 Models for inviscid wakes past bluff bodies. *Fluid Dyn. Res.* **46**, 031407.

ELCRAT, A., FORNEBERG, B., HORN, M. & MILLER, K. 2000 Some steady vortex flows past a circular cylinder. *J. Fluid Mech.* **409**, 13–27.

GALLIZIO, F., IOLLO, A., PROTAS, B. & ZANNETTI, L. 2010 On continuation of inviscid vortex patches. *Physica* D **239**, 190–201.

GANTMACHER, F. R. 1966 *Théorie des Matrices*. Dunod.

IOSILEVSKII, G. & SEGINER, A. 1994 Asymmetric vortex pair in the wake of a circular cylinder. *AIAA J.* **32**, 1999–2003.

JOUKOWSKII, N. E. 1907 On annexed bounded vortices. *Trudy Otd. Fiz. Nauk. Mosk. Obshch. Lyub. Estest. Antr. Etn.* **13** (2), 12–25 (in Russian).

KATZ, J. & PLOTKIN, A. 2001 *Low-speed Aerodynamics*. Cambridge University Press.

LIN, C. C. 1941 On the motion of vortices in two dimensions-I existence of the Kirchoff–Routh function, -II some further investigations on the Kirchoff–Routh function. *Proc. Natl Acad. Sci. USA* **27**, 570–577.

LUGT, H. J. 1985 Vortex flow and maximum principles. *Am. J. Phys.* **53** (7), 649–653.

MELESHKO, V. V. & AREF, H. 2007 A bibliography of vortex dynamics 1858–1956. *Adv. Appl. Mech.* **41**, 197–292.

NEWTON, P. K. 2000 *The N-Vortex Problem*. Springer.

SAFFMAN, P. G. 1992 *Vortex Dynamics*. Cambridge University Press.

SAFFMAN, P. G. & SHEFFIELD, J. S. 1977 Flow over a wing with an attached free vortex. *Stud. Appl. Maths* **57**, 107–117.

SMITH, J. H. B. & CLARK, R. W. 1975 Non-existence of stationary vortices behind a two-dimensional normal plate. *AIAA J.* **13** (8), 1114–1115.

VASCONCELOS, G. L., MOURA, N. M. & SCHAKEL, A. M. J. 2011 Vortex motion around a circular cylinder. *Phys. Fluids* **23**, 123601.

ZANNETTI, L. 2006 Vortex equilibrium in the flow past bluff bodies. *J. Fluid Mech.* **562**, 151–171.

ZANNETTI, L. & FRANZESE, P. 1994 The non-integrability of the restricted problem of two vortices in closed domains. *Physica* D **76**, 99–109.

https://doi.org/10.1017/jfm.2014.418 Published online by Cambridge University Press